

1 Supporting Information to

2

3 **Refined modeling and ^{14}C plateau tuning reveal consistent patterns of glacial and
4 deglacial ^{14}C reservoir ages of surface waters in low-latitude Atlantic**

5

6 Sven Balmer¹⁾, Michael Sarnthein¹⁾, Manfred Mudelsee²⁾³⁾, and Pieter M. Grootes⁴⁾

7

8 ¹⁾Institute of Geosciences, University of Kiel, 24098 Kiel, Germany

9 ²⁾Climate Risk Analysis, Heckenbeck, D-37581 Bad Gandersheim, Germany

10 ³⁾Alfred Wegener Institute, Helmholtz Centre for Polar and Marine Research,

11 27570 Bremerhaven, Germany

12 ⁴⁾Institute for Ecosystem Research, University of Kiel, 24098 Kiel, Germany

13

14

15 **Text S1: XRF-based Ti/Ca measurements**

16 XRF measurements on GeoB 3910-1 were conducted at MARUM, Bremen University,
17 Germany, using an XRF Core Scanner II (AVAAATECH Serial No. 2). XRF data were
18 collected every 4 mm using generator settings of 10 kV, a current of 0.5 mA, and a sampling
19 time of 20 seconds. The surface of the sediment core was covered with a 4-micron thin
20 SPEXCerti Prep Ultralenel foil to avoid contamination of the XRF measurement unit and
21 desiccation of the sediment. The reported data was acquired by a Canberra X-PIPS Silicon
22 Drift Detector (SDD; Model SXD 15C-150-500) with 150 eV X-ray resolution, the Canberra
23 Digital Spectrum Analyzer DAS 1000, and an Oxford Instruments 50W XTF5011 X-Ray tube
24 with Rhodium (Rh) target material. Raw data spectra were processed by the analysis of X-ray
25 spectra by iterative square software (WIN AXIL) package from Canberra Eurisys.

26

27 **Text S2: 1st Derivative**

28 To identify plateaus in the curve of $y = \text{radiocarbon years}$ against $x = \text{core depth}$ in the
29 sedimentary records (Fig. S1) we used the statistical method of Sarnthein et al. [2015]. It is
30 based on the first derivative or slope of the curve over time, $y'(x) = dy(x)/dx$. Plateaus have
31 by definition a slope of zero, while jumps in the curve have large slope values.

32

33 We use a running window, mathematically denoted as kernel, that is running along the x-axis
34 and estimate the slope y' for x equal to the window's center using the points inside the
35 window. This nonparametric technique is called kernel estimation. For example, we may
36 consider the case of the running mean for estimating the zeroth derivative or mean trend,
37 which uses a non-smooth uniform kernel. The first derivative is estimated via the first
38 derivative of the kernel's trend estimate. The kernel method can be adjusted at the boundaries
39 of the x-interval by using a smaller kernel width ("boundary kernel"). Details of the kernel
40 method for derivative estimation are mathematically described by Gasser and Müller [1979];

41 1984], and described in a manner accessible to climatologists by Mudelsee [2014]. Both these
42 papers and the book also contain the mathematical formulas and further references.

43

44 To construct a 1-sigma error band around the slope curve, we used bootstrap resampling
45 [Mudelsee, 2014]. A resample y^* is obtained by

46 (1) calculating the residuals (the differences between trend and data points),
47 (2) resampling point-wise random residuals, and
48 (3) adding the random residuals back to the trend. In case of our data, autocorrelation effects
49 (“memory” of x-values) were negligible. A new first derivative is re-estimated on the
50 resample, yielding $y^*(x)$. The procedure resampling–re-estimation is repeated until $B =$
51 10000 copies of $y^*(x)$ are available. The standard error band results from the standard
52 deviation over the B copies of $y^*(x)$.

53

54 There is room for subjectivity in two dimensions. First, selection of the bandwidth (i.e., the
55 width of the kernel function) determines the bias and variance properties of the slope
56 estimate. Gasser and Müller [1984] defined objective guidelines to optimizing the bandwidth.

57 However, we preferred some degree of ‘under-smoothing’ that is a smaller bandwidth that
58 helps to better uncover the fine details (at the cost of these details being less significant).

59 Second, a threshold value needs to be selected for defining plateaus and jumps in the ^{14}C
60 record. Adopting a threshold value close to zero led to too many plateaus, while a more
61 liberal, larger threshold value clearly led to a better agreement with the plateau boundaries
62 previously identified by visual inspection.

63

64 The 1st derivative confirms the visual tuning of core GeoB 1711-4. Due to low data density
65 we rely on jumps to identify ^{14}C plateau boundaries, except for the top of Plateau 4a. Plateau
66 3 appears smaller than suggested by the Suigetsu reference record (Fig. 2), because of

67 decreasing reservoir ages. An outstanding jump at 210 cm core depth represents the hiatus
68 identified by visual inspection. The 1st derivative of core GeoB 3910-1 is in line with the
69 visual tuning of Plateaus 1a–3. Visual plateau boundaries are verified by jumps (Fig. 2). The
70 plateau tuning of Core KNR 159-5-36GG is strongly confirmed by the 1st derivative, where
71 the half heights of slopes constrain the boundaries of the YD Plateau. All other plateau
72 boundaries are marked by jumps in the core depth – ¹⁴C age relationship. A jump at 185 cm
73 core depth reflects the hiatus identified by visual inspection.

74

75 **Supplementary Text S3: Interspecies Offsets and Inferred Seasonal Record of ¹⁴C**
76 **Signals**

77 Cryptospecies IIb of *G. bulloides sensu* Darling and Wade [2008] is abundant in mid-latitudes
78 and subtropical upwelling belts. It is widely regarded as ‘gourmand’ tracing maximum
79 nutrition of upwelling seasons, but less dependent on changes in sea surface temperature
80 (SST) [Ganssen and Sarnthein, 1983; Sautter and Sancetta, 1992; Fraile et al., 2009]. Thus
81 ¹⁴C variations of *G. bulloides* form a robust record of upwelling changes at Site GeoB1711-4
82 off Namibia, likewise of surface waters nutrient-enriched at Azores Site MD08-3180 during
83 winter and spring [Schwab et al., 2012].

84

85 At Site ODP1002 in the Cariaco Basin (and Cariaco ‘lagoon’ during LGM) most ¹⁴C ages of
86 *G. bulloides* exceed those of *G. ruber* by 100–200 ¹⁴C yr, in rare cases by up to 600 ¹⁴C yr.
87 These anomalies imply that *G. bulloides* forms in waters more enriched in (slightly aged)
88 dissolved inorganic carbon (DIC) than the surface waters where *G. ruber* is living with its
89 symbionts [Hemleben et al., 1989]. During LGM and early HS-1 we find rare groups of
90 samples where ¹⁴C ages of *G. ruber* significantly exceed those of *G. bulloides*. These ‘old’ *G.*
91 *ruber* samples are possibly enriched in reworked specimens admixed from outside to the
92 sediments of the Cariaco lagoon through a shallow inlet channel (~25 m) during times of low

93 sea level stand. In turn, ^{14}C ages analyzed on *G. ruber* and *G. sacculifer trilobus* give
94 perennial records near the equator (GeoB 3910-1), but rather reflect summer conditions in the
95 southern subtropics such as at Site KNR-159-5-36GGC [Ganssen and Sarnthein, 1983;
96 Mulitza et al., 1998].

97

98 At Site MD07-3076, ^{14}C reservoir ages for sections older than 16.5 cal. ka were deduced from
99 ^{14}C ages of *Neogloboquadrina pachyderma* (s). Though probably a different cryptospecies
100 [Darling and Wade, 2008], the ^{14}C signal of South Atlantic *N. pachyderma* (s) may be
101 ascribed to subsurface habitats per analogy to northern high latitudes [Simstich et al., 2003],
102 which in part may explain the elevated reservoir ages shown in Fig. 2. Likewise, the ^{14}C
103 signal of *Globorotalia inflata* may stand for subsurface waters in transitional latitudes
104 [Groeneveld and Chiessi, 2011].

105

106

107 **Supplementary Tables**

108 **Table S1.** Definition of planktic ^{14}C plateaus in new and supplemented ^{14}C records
 109 (defined by visual inspection and confirmed by 1st derivative technique, see Suppl. Text S2)

110

111 Table S1 a) GeoB 1711-4

Plateau No.	TOP		BASE		AVERAGE ^{14}C yr		Pla. res. age [yr] (1.68 σ)	Pla. $\Delta\Delta^{14}\text{C}$ [%] (1.68 s)	ATM fMC
	Depth [cm]	Age [cal yr]	Depth [cm]	Age [cal yr]	GeoB 1711-4	Suigetsu			
1	115	14050	125	14921	13357	12471	880±255	130±40	1.25
2a	127.5	15272	143.5	16050	13844	13426	420±320	67±51	1.325
2b	143.5	16050	150	16400	14543	13850	690±45	111±8	1.35
3	151.5	16900	156.5	17580	15335	14671	660±195	110±28	1.40
Comment:	By comparison with Suigetsu Plateau 3 the short length of Plateau 3 may be explained by a ~200-yr drop in local ^{14}C reservoir age over Plateau 3. Its actual range, 156.5–160.5 cm, is given by a dotted line in Fig. 2.								
4	170	18000	175	18980	16690	15851	840±190	139±33	1.40
5a	177.5	19130	188.5	19600	17399	16670	730±240	126±43	1.45
5b	188.5	19600	195	20150	17936	17007	930±200	158±36	1.45
6a	197.5	20450	208.5	21420	18744	17667	1080±290	186±52	1.475
Comment:	Below Plateau 6a a ^{14}C jump of 2000 yr reflects a hiatus at 210–212 cm depth on top of sediments older than Plateau 7 (23 cal. ka).								

112

113

114 Table S1 b) GeoB 3910-1

Plateau No.	TOP		BASE		AVERAGE ^{14}C yr		Pla. res. age [yr] (1.68 σ)	Pla. $\Delta\Delta^{14}\text{C}$ [%] (1.68 s)	ATM fMC
	Depth [cm]	Age [cal yr]	Depth [cm]	Age [cal yr]	GeoB 3910-1	Suigetsu			
1a	83.5	13640	88.5	13940	12236	12006	230±110	34±2	1.20
1	89.5	14050	105	14921	12680	12471	210±220	32±34	1.25
2a	106	15272	136.5	16050	13602	13426	176±470	29±76	1.325
2b	136.5	16050	143.5	16400	14412	13850	560±180	91±30	1.35
3	145	16900	151.5	17580	15303	14671	630±160	106±27	1.40
Comment	Very low sedimentation rates below Plateau 3 suggest hiatus.								

115

116 Table S1 c) KNR-159-5-36GGC

Plateau No.	TOP		BASE		AVERAGE ^{14}C yr		Pla. res. age [yr] (1.68 σ)	Pla. $\Delta\Delta^{14}\text{C}$ [%] (1.68 s)	ATM fMC
	Depth [cm]	Age [cal yr]	Depth [cm]	Age [cal yr]	KNR-159-5-36GGC	Suigetsu			
YD	70.5	12570	78.5	13000	10848	10747	100±425	15±62	1.20
1a	82.5	13640	88.25	13940	12240	12006	230±310	34±45	1.20
1	88.25	14050	100.5	14921	12650	12471	180±370	28±56	1.25
2a	102.5	15272	131	16050	13600	13426	170±700	28±111	1.325
2b	131	16050	140.75	16400	14190	13850	340±300	56±50	1.35
3	146.5	16900	162.5	17580	15130	14671	460±380	78±65	1.40
4	164.75	18000	176	18980	16600	15851	750±360	125±61	1.40
5a	177.5	19130	182.5	19600	17540	16670	870±120	149±21	1.45
Comment	Two suites of ^{14}C outliers with approximately uniform ^{14}C age each are ascribed to two events of <i>Zoophycos</i> burrowing (Fig.2). Below Plateau 5a a ^{14}C jump of ~1200 yr reflects a hiatus at 182.5–185.5 cm depth.								
7	190.5	22010	-	-	19380	18843	540±140	98±26	1.50

117 **Table S2.** Correlation of ^{14}C ages in GeoB 3910-2 to core depths in GeoB 3910-1 by means
 118 of tuning (XRF-based) high-resolution Ti/Ca records.

119

KIA No.	Raw ^{14}C ages ¹⁾	GeoB 3910-2 ¹⁾		GeoB 3910-1
	^{14}C age [yr]	Depth [cm]	Depth [cm]	
KIA6813	12840±110	88	97	
KIA25825	13550±70	103	111,8	
KIA25824	14000±70	113	129	
KIA6812	15780±110	148	153	
KIA6811	20000±170	173	170	
KIA25822	20580±150	183	175,4	
KIA6808	22480±220	193	201	

120

121

122 **Table S3.** ^{14}C ages, ^{14}C plateaus, and age conversion into calendar ages in three sediment
 123 cores from the tropical and subtropical South Atlantic. The ages of plateau boundaries were
 124 tuned to the calendar ages of (Suigetsu) atmospheric plateau boundaries (see text). In
 125 between, calendar ages were deduced by linear interpolation. Beyond our suite of ^{14}C plateaus
 126 ^{14}C ages (marked in red) were converted using Calib 7.0.4 [Stuiver and Reimer, 1993] with
 127 the Marine13 dataset [Reimer et al., 2013] and extrapolating the reservoir age of the next
 128 closest ^{14}C plateau up- or downcore (accepting potential errors of this extrapolation). Note
 129 that our raw ^{14}C ages were measured in three different ^{14}C laboratories on closely spaced
 130 neighbor samples over an interval of almost two decades. Since neighbor ages closely agree,
 131 the ages probably reflect true ^{14}C concentrations.

132

133 Table S3a) GeoB 1711-4: ^{14}C ages measured on *G. bulloides*.

KIA and UCI Laboratory numbers	Core Depth [cm]	Conventional ^{14}C age [yr]	$\pm\sigma$ error	Plateau No.	Reservoir age [yr]	Calendar age [yr]
UCI 127536	105	12355	±30	-	-	13336
UCI 127537	107.5	12640	±25	-	-	13604
UCI 127538	110	12930	±25	-	-	13928
UCI 127539	112.5	13050	±30	-	-	14056
KIA 47685	115	13220	+70/-60	1	880±255	14050
UCI 127540	117.5	13215	±30	1	880±255	14268
KIA 47679	120	13410	±110	1	880±255	14486
KIA 49307	122.5	13460	±70	1	880±255	14703

KIA 47687	125	13480	+70/-60	1	880±255	14921
KIA 49305	127.5	13660	±70	2a	420±140	15272
KIA 47680	130	13740	±120	2a	420±140	15394
KIA 49399	132.5	13700	±70	2a	420±140	15515
KIA 47688	135	13870	±70	2a	420±140	15637
†KIA 4109	137.5	14060	±60	2a	420±140	15758
KIA 47681	140	14030	±120	2a	420±140	15880
KIA 49308	142.5	13850	±70	2a	420±140	16000
KIA 47689	145	14560	±70	2b	690±45	16131
KIA 49309	147.5	14520	±80	2b	690±45	16265
KIA 47682	150	14550	±130	2b	690±45	16400
KIA 49353	152.5	15500	±90	3	660±195	16971
KIA 47686	155	15170	±90	3	660±195	17174
UCI 140160	156.5	15580	±60	3	660±195	17296
KIA 49354	157.5	15720	±90	-	-	17377
UCI 140161	158.5	15830	±60	-	-	17458
KIA 47683	160	15880	±110	-	-	17580
KIA 49355	162.5	16070	±110	-	-	17685
KIA 47684	165	16220	±160	-	-	17790
KIA 49356	167.5	16390	+100/-90	-	-	17895
KIA 47622	170	16680	±140	4	840±190	18000
KIA48699	175	16700	±90	4	840±190	18980
UCI 140162	176.5	16850	±70	-	-	19070
KIA 49357	177.5	17160	±110	5a	730±240	19130
KIA 47664	180	17590	+ 180/-170	5a	730±240	19237
KIA 49365	182.5	17410	+120/-110	5a	730±240	19344
KIA 47665	185	17610	±190	5a	730±240	19450
UCI 127542	187.5	17225	±40	5a	730±240	19557
KIA 47666	190	17950	±170	5b	930±200	19727
KIA 49366	192.5	17870	±130	5b	930±200	19938
KIA 47667	195	17990	+190/-180	5b	930±200	20150
UCI 140163	196.5	18350	±70	-	-	20330
KIA 49367	197.5	18650	±140	6a	1080±290	20450
KIA 47668	200	18760	±180	6a	1080±290	20670
KIA 49368	202.5	18890	±140	6a	1080±290	20891
KIA 47669	205	18690	±190	6a	1080±290	21111
KIA 49369	207.5	18730	±150	6a	1080±290	21332
KIA 47670	210	19250	±190	-	-	22046
KIA 49398	212.5	21250	±160	-	-	24233
KIA 47671	215	20810	+250/-240	-	-	23755
KIA 49306	217.5	21290	+170/-160	-	-	24272
KIA 47672	220	21290	+280/-270	-	-	24280
KIA 49400	222.5	20200	+150/-140	-	-	23032
KIA 47673	225	21630	+310/-300	-	-	24755
KIA 49401	227.5	21490	+170/-160	-	-	24563
KIA 47674	230	21800	+280/-270	-	-	24916
KIA 49414	232.5	21580	±170	-	-	24683
KIA 47675	235	22640	+370/-350	-	-	25816
KIA 49415	237.5	23510	+220/-210	-	-	26742
KIA 47676	240	23580	+420/-400	-	-	26785

*KIA 555	242.5	18740	± 130	-	-	21348
KIA 47677	245	25040	+490/-460	-	-	28080
KIA 47678	250	25490	+490/-460	-	-	28396
[†] KIA 4110	288	29130	± 240	-	-	31814

*Little et al.. 1997; [†]Vidal et al.. 1999

134
135

136 Table S3b) GeoB 3910-1: ^{14}C ages measured on *G. sacculifer*

KIA and UCI Laboratory numbers	Core Depth [cm]	Conventional ^{14}C age [yr]	1 σ error	Plateau No.	Reservoir age [yr]	Calendar age [yr]
KIA 48760	50.5	9885	± 45	-	-	11071
KIA 48761	60.5	10075	± 45	-	-	11224
KIA 48762	70.5	10550	50/-49	-	-	12127
KIA 48763	80.5	11810	± 50	-	-	13418
KIA 49429	81.5	11890	± 60	-	-	13496
KIA 49430	83.5	12150	± 60	1a	230 \pm 110	13640
KIA 49431	85.5	12360	± 60	1a	230 \pm 110	13760
KIA 49432	87.5	12200	± 60	1a	230 \pm 110	13880
UCI 128554	89.5	12460	± 30	1	210 \pm 220	14050
KIA48764	90.5	12865	± 60	1	210 \pm 220	14106
[†] KIA 6813	97	12840	± 110	1	210 \pm 220	14471
KIA48765	100.5	12620	± 60	1	210 \pm 220	14668
UCI 128555	102.5	12615	± 30	1	210 \pm 220	14781
UCI 128556	104.5	12335	± 35	1	210 \pm 220	14893
KIA 49433	106.5	13840	+80/-70	2a	176 \pm 470	15285
KIA 49527	108.5	13200	± 70	2a	176 \pm 470	15336
KIA48766	110.5	13190	± 70	2a	176 \pm 470	15387
[†] KIA 25825	111.8	13550	± 70	2a	176 \pm 470	15412
UCI 128557	114.5	12855	± 30	2a	176 \pm 470	15489
KIA 49528	117.5	13800	± 70	2a	176 \pm 470	15565
KIA 48767	120.5	13820	± 70	2a	176 \pm 470	15642
KIA 49529	124.5	13760	± 80	2a	176 \pm 470	15744
[†] KIA 25824	129	14000	± 70	2a	176 \pm 470	15859
KIA 49530	133.5	13330	± 70	2a	176 \pm 470	15973
UCI 128558	134.5 – 135.5	13530	± 35	2a	176 \pm 470	15999 – 16024
KIA 49531	137.5	14320	± 80	2b	560 \pm 180	16100
UCI 128559	139.5	14600	± 35	2b	560 \pm 180	16200
KIA 49567	141.5	14250	± 70	2b	560 \pm 180	16300
UCI 128560	142.5	14480	± 40	2b	560 \pm 180	16350
KIA 49568	145.5	15240	± 80	3	630 \pm 160	16943
UCI 128561	147.5	15185	± 40	3	630 \pm 160	17155
KIA 49569	149.5	15370	± 90	3	630 \pm 160	17368
UCI 140169	151.5	15420	± 50	3	630 \pm 160	17580
[†] KIA 6812	153.4	15780	± 110	-	-	18416
UCI 140170	153.5	15750	± 45	-	-	18379
UCI 144777	154.5	15795	± 40	-	-	18426
KIA 49570	156.5	16640	± 100	-	-	19324
UCI 140171	157.5	16700	± 60	-	-	19391
UCI 144778	158.5	16765	± 45	-	-	19497
KIA 49571	161.5	17590	± 100	-	-	20447

UCI 140172	163.5	17670	±70	-	-	20550
UCI 144779	164.5	18090	±60	-	-	21068
KIA 49572	165.5	18280	±120	-	-	21335
UCI 140174	167.5	18480	±70	-	-	21635
KIA 49573	170.5	19050	±120	-	-	22293
UCI 140173	172.5	19220	±70	-	-	22447
KIA 49574	174.5	19520	+140/-130	-	-	22733
†KIA 6811	175.4	20000	±170	-	-	23310
UCI 132989	182.5	20510	±90	-	-	23923
†KIA 25822	183	20580	±150	-	-	24000
†KIA 6808	201	22480	±220	-	-	25908

†Jaeschke et al., 2007; ^{14}C ages from GeoB 3910-2. Depths are correlated based on tuned Ti/Ca ratios (see Table S2)

137
138

139 Table S3 c) KNR 159-5-36GGC: ^{14}C ages measured on *G. ruber*

UCI and NOS Laboratory numbers	Core Depth [cm]	Conventional ^{14}C age [yr]	1 σ error	Plateau No.	Reservoir age [yr]	Calendar age [yr]
*OS-27350	60	9450	±50	-	-	10644
†UCI 64771	60.5	9115	±20	-	-	10232
*OS-25479	64	10750	±90	-	-	12590
†UCI 92828	65.5	9425	±20	-	-	10620
†UCI 77922	67.5	10425	±25	-	-	12120
*OS-23210	68	10600	±45	-	-	12469
†UCI 64783	70.5	10705	†30	YD	100±425	12570
UCI 144785	72.5	10860	±45	YD	100±425	12640
†UCI 77923	75.5	10990	±25	YD	100±425	12745
UCI 144786	77.5	10835	±35	YD	100±425	12815
*OS-23211	80	11400	±50	-	-	13161
UCI 140175	80.5	12260	±90	-	-	13245
†UCI 64784	80.5	11485	±30	-	-	13245
UCI 144787	82.5	12200	±35	1a	230±310	13640
†UCI 77924	85.5	12460	±30	1a	230±310	13797
UCI 140176	87.5	12105	±40	1a	230±310	13901
*OS-23212	88	12200	±50	1a	230±310	13927
UCI 144788	88.5	12770	±60	1	180±370	14068
†UCI 64785	90.5	12705	±35	1	180±370	14210
*OS-22677	92	12450	±60	1	180±370	14317
UCI 144789	92.5	12600	±80	1	180±370	14352
†UCI 77925	95.5	12275	±30	1	180±370	14565
UCI 140177	97.5	6925	±25	1	180±370	14708
†UCI 64786	100.5	12710	±30	1	180±370	14921
UCI 140178	102.5	13235	±50	2a	170±700	15272
*OS-23318	104	13550	±60	2a	170±700	15313
UCI 144790	104.5	13560	±60	2a	170±700	15327
†UCI 77926	105.5	13295	±35	2a	170±700	15354
†UCI 64787	110.5	13465	±35	2a	170±700	15490
*OS-23317	112	13650	±60	2a	170±700	15331
†UCI 77927	115.5	13630	±30	2a	170±700	15627
UCI 144791	117.5	13945	±50	2a	170±700	15682
†UCI 64788	120.5	13350	±40	2a	170±700	15763

UCI 140179	122.5	13740	±50	2a	170±700	15818
UCI 144794	123.5	11800	±55	2a	170±700	15845
†UCI 77928	125.5	13765	±35	2a	170±700	15900
UCI 140181	127.5	11360	±45	2a	170±700	15956
†UCI 64789	130.5	13955	±35	2a	170±700	16036
UCI 144795	132.5	11905	±45	2b	340±300	16104
†UCI 92829	134.5	14340	±70	2b	340±300	16176
†UCI 64790	140.5	14045	±35	2b	340±300	16391
*OS-23213	141	14850	±120	-	-	16421
†UCI 77929	142.5	11975	±25	-	-	16549
UCI 140182	144.5	13500	±60	-	-	16720
†UCI 92906	146.5	15240	±90	3	460±380	16890
*OS-22678	148	12350	±65	3	460±380	16955
†UCI 64791	150.5	15500	±70	3	460±380	17063
UCI 140183	155.5	14090	±60	3	460±380	17278
UCI 140184	157.5	15220	±90	3	460±380	17364
†UCI 64792	160.5	12055	±30	3	460±380	17494
UCI 144796	162.5	15590	±110	3	460±380	17580
UCI 140185	165.5	16790	±120	4	750±360	18066
UCI 144797	166.5	16480	±140	4	750±360	18155
†UCI 64793	170.5	14365	±35	4	750±360	18510
UCI 144798	173.5	13450	±60	4	750±360	18775
UCI 140186	175.5	16530	±90	4	750±360	18953
UCI 140187	177.5	17520	±100	5a	870±120	19130
†UCI 77930	180.5	17510	±60	5a	870±120	19412
†UCI 92910	182.5	17590	±80	5a	870±120	19600
†UCI 77931	185.5	18780	±70	-	-	20504
UCI 140188	187.5	18930	±120	-	-	21106
†UCI 77932	190.5	19340	±60	7	540±140	22010
UCI 140189	195.5	19420	±100	-	-	22723
† UCI 77933	200.5	15525	±50	-	-	18210

*Came et al.. 2003; †Sortor and Lund. 2011

140
141

142 **Table S4.** Age control points used for calculation of sedimentation rates.

143 Table S4a) GeoB 1711-4

¹⁴ C Plateau boundaries used as tie points	Calendar age [yr]	Core depth [cm]	Sedimentation rate [cm/kyr]
Top 1 – Base 1	14050 - 14921	115 – 125	11.4
Base 1 – Base 2a / Top 2b	14921 - 16050	125 – 143.5	16.3
Top 2b – Top 3	16050 - 16890	143.5 – 151.5	9.5
Top 3 – Base 3	16890 - 17580	151.5 – 160	12.3
Base 3 – Base 4	17580 - 18980	160 – 175	10.7
Base 4 – Base 5a / Top 5b	18980 - 19600	175 – 188.5	21.7
Top 5b – Base 5b	19600 - 20150	188.5 – 208.5	11.8
Base 5b – Base 6a	20150 - 21420	195 – 208.5	10.6

144

145
146
147
148

Table S4b) GeoB 3910-1

¹⁴ C Plateau boundaries used as tie points	Calendar age [yr]	Core depth [cm]	Sedimentation rate [cm/kyr]
Top 1a– Base 1a	13640 - 13940	83 – 88.5	16.7
Base 1a – Base 1	13940 - 14921	88.5 – 105	16.8
Base 1 – Base 2a / Top 2b	14921 - 16050	105– 136.5	27.9
Top 2b – Top 3	16050 - 16890	136.5– 145	10.1
Top 3 – Base 3	16890 - 17580	145 – 151.5	9.4

149

150 Table S4c) KNR-159-5-36GGC

¹⁴ C Plateau boundaries used as tie points	Calendar age [yr]	Core depth [cm]	Sedimentation rate [cm/kyr]
Top YD– Base YD	12570 - 13000	70 – 78.5	18.6
Base YD – Base 1a	13000 - 13940	78.5 – 88.25	10.3
Base 1a – Base 1	13940 - 14921	88.25– 100.5	12.4
Base 1 – Base 2a / Top 2b	14921 - 16050	100.5– 131	27
Top 2b – Top 3	16050 - 16890	131 – 146.5	18.4
Top 3 – Top 4	16890 – 18000	146.5 – 164.75	16.4
Top 4 – Top 5a	18000 – 19130	164.75 – 177.5	11.2
Top 5a – Base 5a	19130 - 19600	177.5 – 182.5	10.6

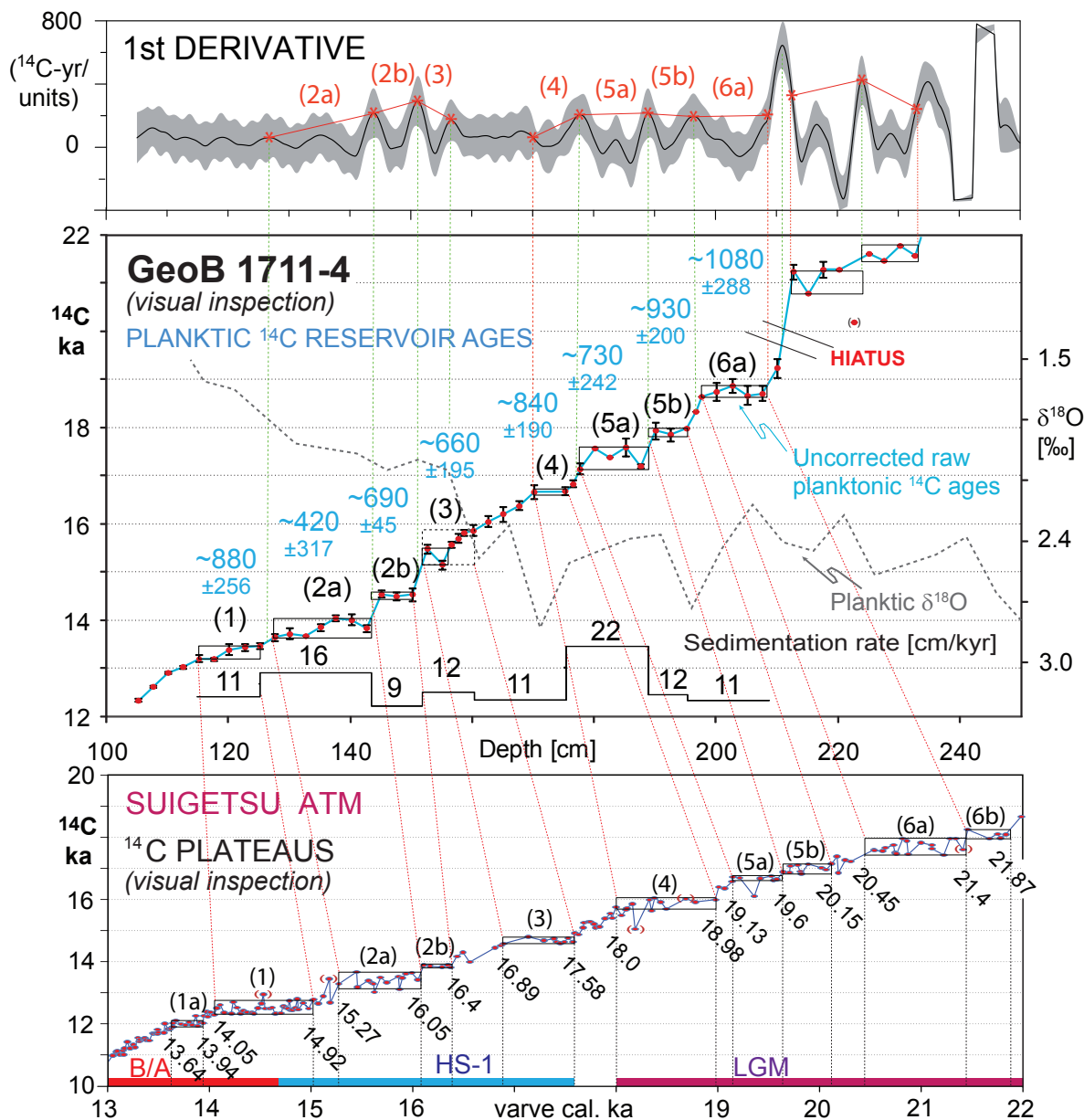
151

152

153 **Supplementary figures**

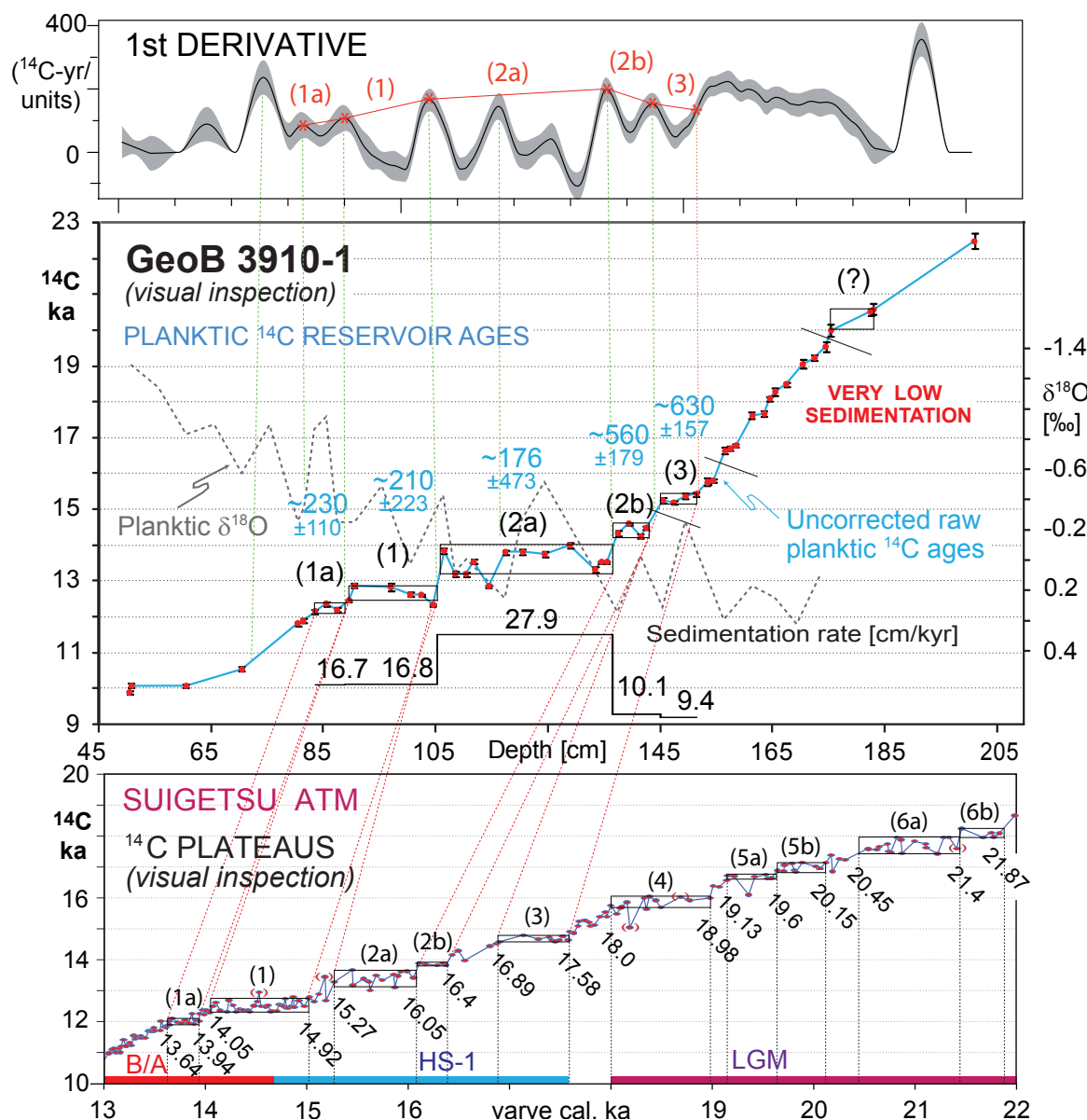
154 **Figure S1.** Mid panel: Planktic ^{14}C records of cores GeoB1711-4, GeoB3910-1, KNR-159-5-
155 36 GGC (Table S3), and MD07-3076 plotted vs. core depth, moreover, vs. planktic
156 (*GeoB1711*: Little et al., 1997; *GeoB3910*: own data) or benthic $\delta^{18}\text{O}$ records (KNR159-5-36:
157 Curry and Oppo, 2005) or planktic species counts (MD07-3076: Skinner et al., 2010), finally,
158 vs. sedimentation rates. Planktic ^{14}C plateaus (horizontal boxes) and/or ^{14}C jumps are tuned to
159 atmospheric (atm) ^{14}C plateau suite of Lake Suigetsu (bottom panel, [Bronk Ramsey et al.,
160 2012]), with varve-based calendar ages given below. Local planktic reservoir ages (in blue)
161 result from difference between the average raw ^{14}C ages of planktic ^{14}C plateaus measured in
162 a core and the ^{14}C age of equivalent atmospheric ^{14}C plateaus numbered 1–7 (numbers in
163 brackets). Topmost panels show 1st derivative units (^{14}C yr per cm core depth; bandwith: 1/3
164 optimum smoothing at 2.5 cm sample spacing) and 1-sigma uncertainty range (shaded). High
165 values indicate ^{14}C jumps (linked by green correlation lines). Low values show ^{14}C plateaus
166 (correlation lines and numbers in red) constrained at “half-height” by asterisks. YD =
167 Younger Dryas, B/A = Bølling-Allerød, H1 = Heinrich Stadial 1, LGM = Last Glacial
168 Maximum. Sedimentation rates interpolated between plateau boundary ages (Table S4).
169
170

171 **Figure S1a)**

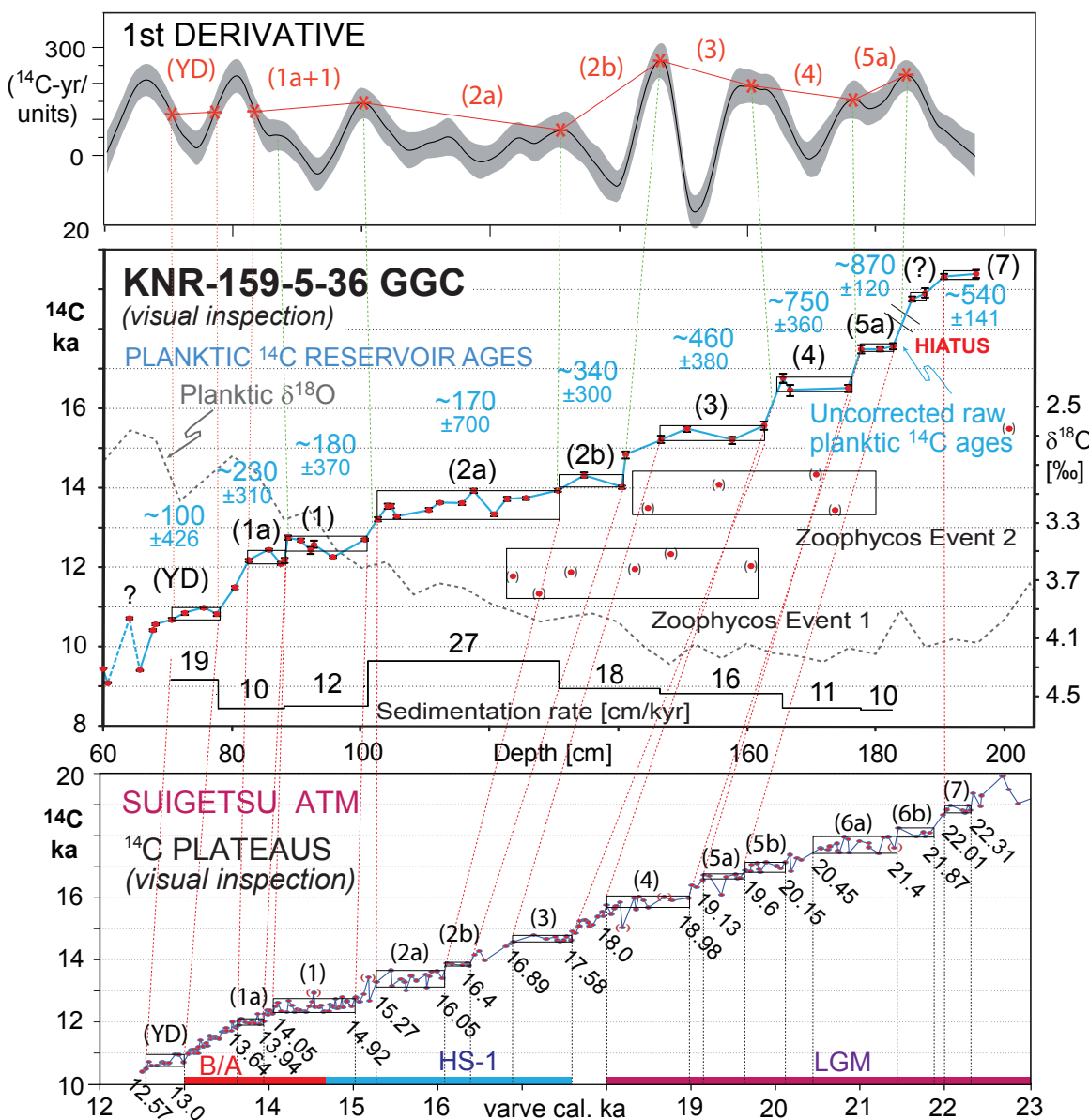


172

173 **Figure S1b)**



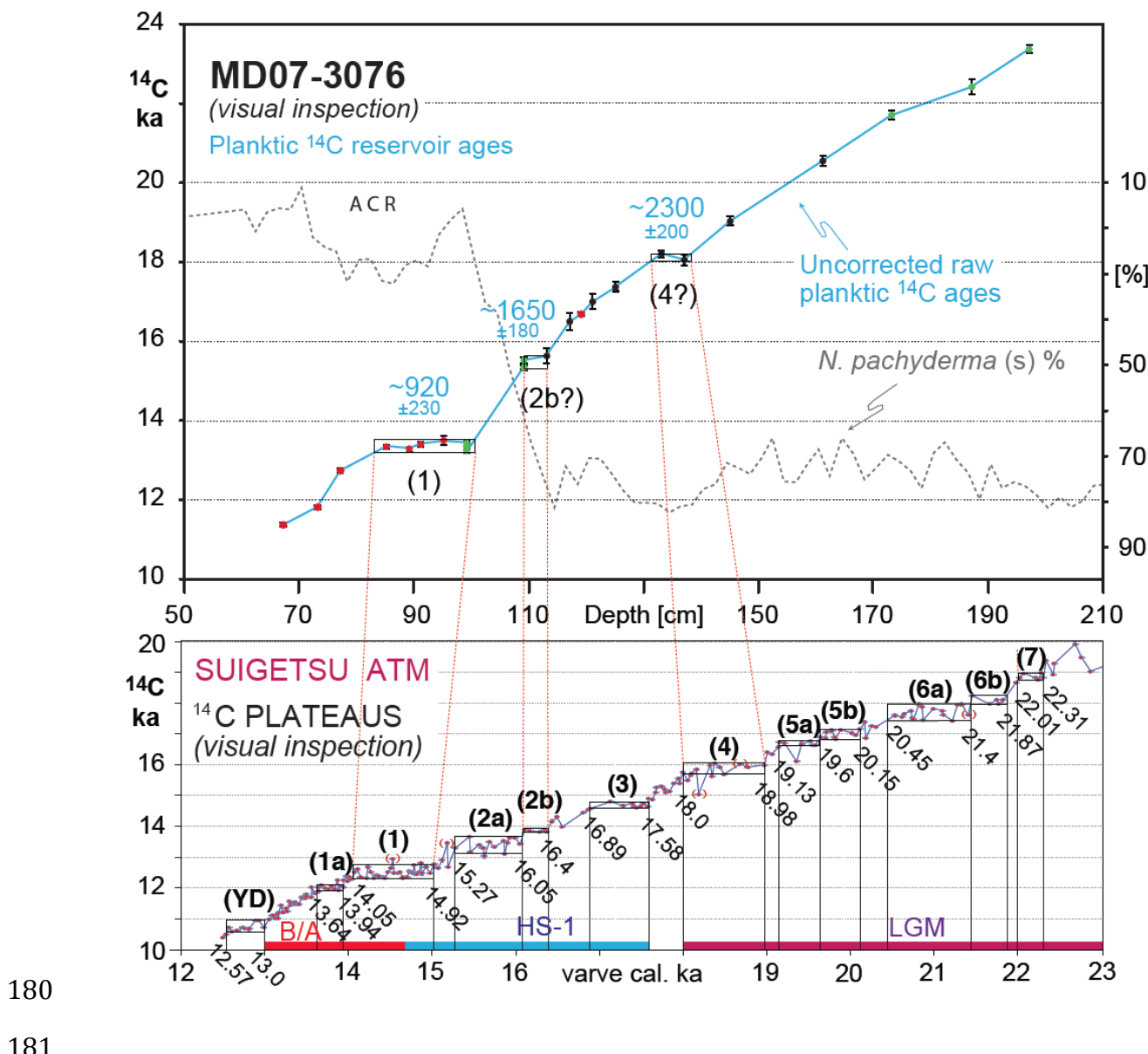
176 Figure S1c)



177

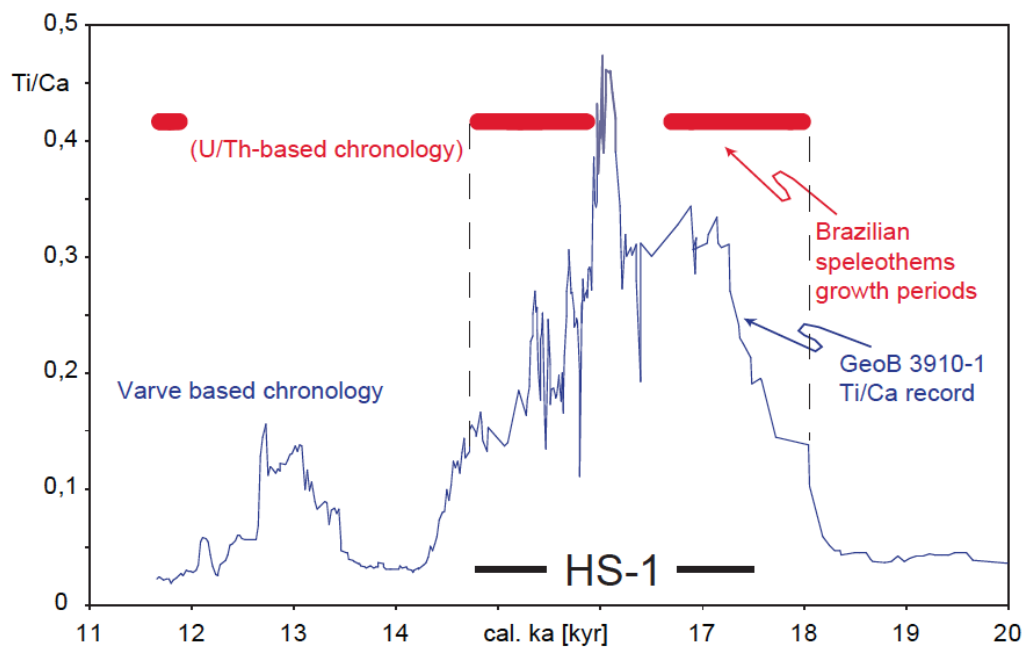
178

179 Figure S1d)



182 **Figure S2.** Deglacial Ti/Ca record of Core GeoB3910-1 vs. Suigetsu varve-based calendar
183 age [Bronk Ramsey *et al.*, 2012], compared to growth periods of speleothems in Northeast
184 Brazil [Wang *et al.*, 2004].

185



186

187